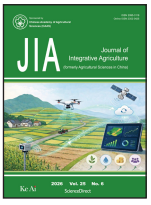
Journal of Integrative Agriculture 2026, 25(6): 2449–2461

Available online at ScienceDirect

Journal of Integrative Agriculture



RESEARCH ARTICLE

The conserved *Xanthomonas* effector XopM targets allene oxide synthase OsAOS3 and interferes with jasmonate-mediated defense in rice

Ying Li, Linlin Liu, Qi Wang, Yong Wang, Jiali Yan, Moein Khojasteh, Syed Mashab Ali Shah, Zhengyin Xu#, Gongyou Chen#

Shanghai Collaborative Innovation Center of Agri-Seeds/State Key Laboratory of Microbial Metabolism, School of Agriculture and Biology, Shanghai Jiao Tong University, Shanghai 200240, China

Highlights

- XopM contributes to *Xoo* virulence in rice.
- XopM targets OsAOS3 to modulate JA biosynthesis.
- XopM suppresses JA-mediated defense to promote infection.

Abstract

Bacterial blight (BB) of rice caused by the phytopathogenic bacterium *Xanthomonas oryzae* pv. *oryzae* (*Xoo*) is a disease of global importance. *Xoo* utilizes the type III secretion system (T3SS) and its effectors for virulence, and XopM is a conserved T3SS effector in *Xanthomonas* spp. However, the virulence function of XopM is largely unknown. In this study, we show that XopM contributes to *Xoo* virulence in rice. We demonstrate that XopM interacts with allene oxide synthase OsAOS3, a key enzyme involved in jasmonic acid (JA) biosynthesis. The expression levels of *OsAOS3* and three homologues of *OsAOS* were elevated after *Xoo* infection. Knockout mutants of *OsAOS3* exhibited decreased JA accumulation and reduced resistance to *Xoo* and *X. oryzae* pv. *oryzicola*. Moreover, JA-related defense genes were downregulated in *osaos3* mutants during *Xoo* infection. Based on our results, we propose a model showing how XopM hijacks OsAOS3 to interfere with JA-mediated defenses, leading to a suppression of rice immunity. Our findings reveal a novel virulence strategy where *Xanthomonas* pathogens interfere with the JA pathway and modulate the host defense response.

Keywords: *Xanthomonas*, XopM, allene oxide synthase, jasmonic acid, plant immunity

1. Introduction

Pathogens utilize a variety of virulence factors to subvert plant immunity and cause disease (Boller and He 2009; Deslandes and Rivas 2012; Dou and Zhou 2012), and plants have gradually evolved a complex, multilayered defense system for pathogens (Tyler 2017). In the ongoing arms race between plants and pathogens, pattern-triggered immunity (PTI) represents the first and most conservative layer of plant innate immunity, which is triggered by recognizing pathogen-associated molecular patterns (PAMPs) through pattern-recognition receptors (PRRs) (Dodds and Rathjen 2010). Consequently, pathogens have evolved virulence "effectors" to suppress PTI, thus leading to effector-triggered susceptibility (ETS) (Jones and Dangl 2006). In response, plants have developed cytoplasmic resistance (R) proteins that enable them to recognize effectors and initiate a second layer of immunity known as effector-triggered immunity (ETI) (Yuan *et al.* 2021; Ngou *et al.* 2022).

Xanthomonas oryzae pv. *oryzae* (*Xoo*), the causal agent of bacterial blight (BB) of rice, secretes various effectors into host cells *via* the type III secretion system (T3SS). The effectors are divided into two groups: transcription activator-like effectors (TALEs) and non-TALE/*Xanthomonas* outer proteins (Xops) (Furutani *et al.* 2009; White *et al.* 2009; Song and Yang 2010). TALEs have been identified as cross-kingdom transcription factors that activate the expression of corresponding susceptibility (*S*) or resistance (*R*) genes in host plants, which induce ETS or ETI (Xu *et al.* 2022). There

Received 3 June 2024; Received in revised form 25 June 2024; Accepted 4 July 2024; Available online 22 August 2024
#Correspondence Gongyou Chen, E-mail: gyouchen@sjtu.edu.cn; Zhengyin Xu, E-mail: xuzy2015@sjtu.edu.cn

© 2026 CAAS. Publishing services by Elsevier B.V. on behalf of KeAi Communications Co. Ltd. This is an open access article under the CC BY-NC-ND license (http://creativecommons.org/licenses/by-nc-nd/4.0/). Peer review under responsibility of Editorial Board of *Journal of Integrative Agriculture*.
doi: 10.1016/j.jia.2024.08.018

are several major TALEs that play a dominant role in *Xoo* virulence, including PthXo1 from the Philippine strain *Xoo* PXO99^{A} (Chen *et al.* 2010).

The T3SS effectors secreted by *Xanthomonas* spp. have been classified into 39 families based on sequence similarities (Wang *et al.* 2016), and 26 non-TALEs have been identified in *Xoo* PXO99^{A} (http://www.biopred.net/xanthomonas/t3e.html). TAL effectors act as transcription factors and are involved in the activation of susceptibility and resistance genes in rice. A previous study reported that a *tal*-free PH strain derived from PXO99^{A} was generated as a strain to explore the function of TALEs (Ji *et al.* 2016). In contrast to TALEs, the biochemical roles of many non-TALEs are not well-understood due to their redundancy and subtlety (Song and Yang 2010). Several characterized non-TALEs are known to function in *Xoo* virulence by suppressing the immune response of host plants (Sinha *et al.* 2013; Long *et al.* 2018; Deb *et al.* 2020). For example, XopR from *Xoo* strain MAFF311018 targets the receptor-like kinase BIK1 and suppresses stomatal closure (Wang *et al.* 2016), thereby creating a natural entry for bacterial cells. XopZ was identified as a conserved effector for full virulence (Song and Yang 2010), and it was shown to repress PTI in tobacco and rice (Long *et al.* 2018). XopI from the *Xoo* BAI3 strain suppressed systemic acquired resistance (SAR) by mimicking and hijacking the ubiquitin proteasome system in rice (Ji *et al.* 2020). XopY targets the rice receptor-like cytoplasmic kinase OsRLCK185 and disrupts signal transduction (Yamaguchi *et al.* 2013). These findings indicate that the Xop effectors manipulate different components of the plant immune system to cause disease.

xopM$_{Xcv}$ (GenBank accession no. XCV0442) was initially cloned and identified as a gene encoding a T3SS effector in *Xanthomonas campestris* pv. *vesicatoria* (*Xcv*) strain 85–10 (Schulze *et al.* 2012). XopM$_{Xcv}$ triggered cell death and inhibited mitogen-activated protein kinase (MAPK)-mediated cell death in *Nicotiana benthamiana* (Schulze *et al.* 2012; Teper *et al.* 2015). *Xoo* strain PXO99^{A} contains a gene homologous to *xopM*$_{Xcv}$ (http://www.biopred.net/xanthomonas/t3e.html); however, the function of XopM in *Xoo* is unclear.

Phytohormones are low molecular weight compounds that influence plant metabolism and reproductive development; furthermore, they play a pivotal role in mediating defense responses during the host–pathogen interaction (Spoel and Dong 2008; Pieterse *et al.* 2012; Ruan *et al.* 2019; Bittner *et al.* 2022). Once conserved pathogen molecules are recognized by plasma membrane localized PRRs, the defense systems associated with the phytohormones jasmonic acid (JA), salicylic acid (SA), and ethylene (ET) are rapidly activated (Campos *et al.* 2014). The JA pathway is a key component of the plant–pathogen interaction (Major *et al.* 2017) and modulates crosstalk with other phytohormones, including SA, ET, gibberellin (GA), and phytochrome (Zhang *et al.* 2019; Meng *et al.* 2020).

Jasmonates are a class of oxylipin phytohormones (Wasternack and Hause 2013). JA biosynthesis is initiated in the chloroplast, primarily from α-linolenic acid (18:3) or free fatty acids (Ruan *et al.* 2019). The first step occurs at the chloroplast membrane where 13-lipoxygenase LOX catalyzes the conversion of α-linolenic acid to (13S)-hydroperoxy octadecatrienoic acid (13-HPOT) (Ruan *et al.* 2019; Li *et al.* 2022). Next, allene oxide synthase (AOS) and allene oxide cyclase (AOC) catalyze the coupled dehydration-cyclization of 13-HPOT, which leads to the production of 12-oxo-phytodienoic acid (OPDA). OPDA is transported from chloroplasts to the peroxisomes for further biosynthesis.

AOS is a key enzyme in JA biosynthesis and regulates disease resistance (Gomi *et al.* 2010; Ruan *et al.* 2019). In rice, the *AOS* gene family consists of four members, *OsAOS1*, *OsAOS2*, *OsAOS3*, and *OsAOS4*. In rice seedlings, *OsAOS* transcription is regulated by phytochrome, and expression levels of *OsAOS1* and *OsAOS4* were elevated in response to red and far-red light, respectively (Haga and Iino 2004). *OsAOS2* transcription was upregulated during rice infection by the fungal pathogen *Magnaporthe grisea*, and this led to the expression of pathogenesis-related (PR) genes that function in defense (Mei *et al.* 2006). Several lines of evidence indicate that the JA signaling pathway functions in plant immunity (Campos *et al.* 2014). For example, group 1 GH3 (Gretchen Hagen 3) genes positively regulated rice resistance to *Xoo* by modulating JA homeostasis and the transcription of JA-responsive genes (Hui *et al.* 2019). In rice, the exogenous application of JA enhanced resistance to *Xoo*, and the jasmonate ZIM-domain protein OsJAZ8 had an important role in JA-mediated resistance (Yamada *et al.* 2012). Correspondingly, many bacterial pathogens have evolved effector proteins that manipulate plant hormones to enable pathogen proliferation (Hu *et al.* 2022; Roussin-Léveillée *et al.* 2022).

In this study, we demonstrate that the effector XopM contributes to *Xoo* virulence in rice and interacts with the allene oxide synthase OsAOS3. The expression of *OsAOS3* was upregulated during *Xoo* infection, and *osaos3* knockout mutants exhibited lower levels of JA and increased susceptibility to *Xoo*. Our findings reveal a novel virulence strategy in the *Xoo*-rice interaction, where XopM hijacks OsAOS3 to interfere with JA-mediated defense responses in rice.

2. Materials and methods

2.1. Bacterial strains and plant materials

The bacterial strains and plasmids used in this study are listed in Appendix A. *Escherichia coli* strains were cultured in Luria-Bertani (LB) medium at 37°C (Tuttle *et al.* 2021). *Agrobacterium* was cultivated at 28°C in LB. *Xanthomonas* strains were grown at 28°C in nutrient broth without agar (NB) (1% peptone, 0.5% yeast extract, 1% sucrose), NB without sucrose (NBN), NB with 1.5% agar (NA), NA without sucrose (NAN), and NA with 10% sucrose (NAS) (Li *et al.* 2011). Yeast cells were grown in yeast extract potato dextrose (YPD) and synthetic dropout media at 28°C (Lin and Lai 2017). Media formulations were supplemented with the following antibiotics: 25 μg mL^{-1} rifampicin, 100 μg mL^{-1} ampicillin, 25 μg mL^{-1} kanamycin, and 40 μg mL^{-1} spectinomycin.

Rice plants (*Oryza sativa* L.) were grown in field plots and greenhouses for pathogenicity assays, and the latter were maintained at 28°C with a 12 h light/dark photoperiod. The rice lines used in this study were japonica cultivars Kitaake

and Nipponbare, and the latter was used as a background for generating *OsAOS3* mutant lines. Tobacco plants (*N. benthamiana*) were cultivated in growth chambers with a 16 h light/8 h dark photoperiod at 22°C.

2.2. Plasmid constructs and DNA manipulations

The introduction of *pthXo1* into *Xoo* PH was accomplished by first cloning *pthXo1*-flanking fragments (2,003 and 771 bp) into *Sma*I/*Xba*I-digested pKMS1 (Appendix B). Next, *pthXo1* was cloned between the two flanking fragments as a 3.9-kb *Bam*HI fragment to generate pKMS1-PthXo1; this was introduced into *Xoo* PH by electroporation to generate *Xoo* PH-PthXo1 as described previously (Ji *et al.* 2016). Briefly, the pKMS1-PthXo1 construct was introduced into *Xoo* PH by electroporation and cultured on NAN+kanamycin at 28°C for 3 d. The transformants that grew on NAN+kanamycin but not NAS were selected and cultured in NBN with agitation at 28°C for 12 h. Cultures were plated on NAS at 28°C for 3–4 d. Individual colonies that grew on NAS but showed kanamycin sensitivity were screened for the presence of *pthXo1* using primers TALE-CF/PthXo1-XbaI-R (Appendix C). The conserved domain deletion assays were performed using the Fast MultiSite Mutagenesis System (TransGen Biotech, Beijing, China).

2.3. Construction of non-TALE mutants in *Xoo* PH-PthXo1

To generate *xopM* deletion mutants, two pairs of primers, XopM-LF/XopM-LR and XopM-RF/XopM-RR (Appendix C), were used to amplify the flanking DNA of *xopM* using genomic DNA from *Xoo* PXO99^{A} as the template. The flanking fragments (616 and 909 bp) were digested and inserted into *Sma*I/*Xba*I-digested pKMS1 (Appendix D) and confirmed by Sanger sequencing (Tsingke Biotechnology Co., Ltd., Beijing, China). The resulting plasmid was transformed into *Xoo* PH-PthXo1 and cultured on NAN medium containing kanamycin at 28°C for 3 d. Single colonies were cultured in NBN with shaking for 12 h at 28°C. *Xoo* cells were then dispensed in 10-fold serial dilutions (10^{-1}, 10^{-2}, and 10^{-3}) and cultured on NAS medium. Kanamycin-sensitive colonies were chosen for PCR confirmation with primers XopM-LF/XopM-RR (Appendix C). The same procedure was performed to delete the other 25 genes encoding non-TALE effectors in *Xoo* PH-PthXo1.

2.4. Generation of OsAOS3 mutant rice by CRISPR/Cas9

OsAOS3 was edited in Nipponbare rice using the CRISPR/Cas9 system as described previously (Zhou *et al.* 2014). Briefly, a specific gRNA was designed using guide design resources (https://zlab.squarespace.com/guide-design-resources). Two gRNA oligomers (OsAOS3-oligo-F/OsAOS3-oligo-R) were synthesized by Tsingke Biotech (Shanghai, China); these oligomers were dimerized, inserted into pENTR4-gRNA4, and then ligated into pBY02-Cas9 using the Gateway™ LR Clonase™ II Kit (Thermo Fisher Scientific) to generate the construct pCas9-gRNA4-AOS3.

The pCas9-gRNA4-AOS3 construct was introduced into Nipponbare rice by *Agrobacterium*-mediated transformation, which was a service provided by BioRun (Wuhan, China). Extraction of genomic DNA was performed using the cetyl trimethylammonium bromide (CTAB) method. The sequences targeted for modification were amplified from genomic DNA using primers OsAOS3-F and OsAOS3-R (Appendix C). Gene editing was confirmed by Sanger sequencing.

2.5. Pathogenicity assays

Xoo PXO99^{A} and *Xoc* BLS256 were cultured overnight in NB medium, and bacterial cells were harvested by centrifugation at 5,000 r min^{-1} for 3 min and washed two times in water. Rice plants were inoculated with *Xoo* PXO99^{A} (OD_{600}=0.8) at the booting stage using the leaf-clipping method (Ji *et al.* 2016). Two-week-old rice was inoculated with *Xoc* BLS256 (OD_{600}=0.8) by the stab-inoculation method (Pan *et al.* 2018). *Xoo* and *Xoc* disease lesions were measured and photographed at 14 and 7 d after inoculation, respectively.

2.6. Subcellular localization assays

Subcellular localization assays were performed as described previously (Kokkirala *et al.* 2010). Briefly, the target coding sequences were amplified by PCR using the specific primers (Appendix C). Purified PCR products were inserted into pC1300-GFP. These constructs were transformed into *Agrobacterium* GV3101 and introduced into tobacco leaves by agroinfiltration. The empty vector, pC1300-GFP, was used as a positive control. Fluorescent signals were detected using a Leica TCS SP5-II Confocal Microscope (Leica Microsystems, Wetzlar, Germany) at 36 h post-inoculation (hpi). Images were captured at 488 nm (excitation) and 505–550 nm (emission), and chlorophyll autofluorescence was detected at 640–735 nm.

Subcellular localization assays in rice protoplasts were performed as described previously (Zhai *et al.* 2019). The coding sequences of $XopM_{Xoo}$ and $XopM_{Xoc}$ were inserted into pRTVcGFP. Rice protoplasts were isolated from seedling sheaths and stems, and the recombinant plasmids were transformed into protoplasts by polyethylene glycol-mediated DNA transfection as described previously (Zhai *et al.* 2019). The transfected cells were incubated in the dark for 22 h at 28°C and then observed by confocal microscopy.

2.7. Yeast two-hybrid assays

The Matchmaker™ GAL4 two-hybrid system (Clontech, CA) was used to screen for rice proteins that interact with XopM. Briefly, *xopM* was amplified from genomic DNA of PXO99^{A} and inserted into pGBKT7 as a bait. Competent cells of yeast strain AH109 were co-transformed with pGBKT7-$XopM_{Xoo}$ and the rice cDNA library; these cells were then cultured on SD/–Leu–Trp–His medium (lacking tryptophan, leucine, and histidine) at 28°C for 3 d. The colonies were then transferred to SD/–Leu–Trp–His–Ade (lacking leucine, tryptophan, histidine and adenine) medium containing 20 mg mL^{-1} X-α-GAL. Transformed yeast colonies were identified by PCR using primers T7/3AD (Appendix C), and PCR products were subjected to Sanger sequencing. *OsAOS3* was amplified from rice cDNA inserted into pGADT7. The interaction of

XopM and OsAOS3 was confirmed in yeast cells cultured on SD/–Leu–Trp–His–Ade medium containing 20 mg mL^{-1} X-α-GAL.

2.8. Split luciferase complementation assays

Split luciferase complementation assays were performed as described previously (You *et al.* 2016). Briefly, $xopM_{Xoo/Xoc}$ and *OsAOS1–4* were cloned in pCAMBIA-35S-nLuc and pCAMBIA-35S-cLuc, respectively. Constructs were transformed into *Agrobacterium* GV3101 and cultured overnight in LB with kanamycin and rifampicin. Bacterial cells were harvested and resuspended in *Agrobacterium* induction buffer, mixed with GV3101 expressing p19 protein, and induced for 2–3 h at 28°C in darkness. The suspensions were infiltrated into tobacco leaves, and luciferase activity was measured at 48 hpi with the Luciferase Reporter Gene Assay Kit (Yeasen Biotechnology, Shanghai, China).

2.9. Southern blots

Genomic DNA was extracted from $PXO99^A$ and PH-PthXo1 with the AxyPrep Bacterial Genomic DNA Miniprep Kit (Axygen, Suzhou, China). DNA samples (10 μg) were digested with *Bam*HI at 37°C for 4 h, separated in 1.3% agarose gels at 70 V for 20 h and transferred to nylon membranes (Millipore, USA). The *pthXo1* probe (2,892 bp; GenBank accession no. AY495676) was labeled with digoxigenin. The labelling, hybridization, and detection steps were conducted with the DIG-High Prime DNA Labelling and Detection Starter Kit I (Roche, Switzerland) using protocols recommended by the manufacturer.

2.10. Western blots

Western blots were used to detect proteins in tobacco as described previously with minor modifications (Yu *et al.* 2022). In brief, *Agrobacterium* GV3101 harboring the constructs $pXopM_{Xoo}$-nLuc, $pXopM_{Xoc}$-nLuc, and pcLuc-OsAOS1 were infiltrated into *N. benthamiana* leaves. Tobacco leaves were collected at 48 h after agroinfiltration and ground in liquid nitrogen. The macerated leaves were incubated with 200 μL protein extraction buffer (50 mmol L^{-1} Tris-HCl, pH 7.5, 150 mmol L^{-1} NaCl, 1 mmol L^{-1} EDTA, 5 mmol L^{-1} DTT, and 1 mmol L^{-1} PMSF) for 20 min at 4°C with agitation and centrifuged. Supernatants (80 μL) were transferred into new tubes and 20 μL 5×SDS buffer was added; the mixture was then boiled in water for 5 min. Proteins were separated on 10% SDS-PAGE gels and transferred to PVDF membranes for immunoblotting. Anti-Luc (Sigma, USA) was used as the primary antibody. Goat anti-rabbit immunoglobulin G (H+L) (Transgen Biotech, Beijing, China) was used to detect anti-FLAG antibodies, and proteins were visualized with the LumiBest Western Kit (Share-Bio, Shanghai, China).

2.11. Preparation and purification of recombinant proteins

The coding sequences of *xopM* and *OsAOS3* were amplified and cloned into pET41a and pET30a, respectively. These constructs were introduced into *E. coli* BL21 by heat shock, and cells were cultured overnight at 37°C in 2 mL LB supplemented with kanamycin. Overnight cultures (400 μL) were inoculated into 40 mL of LB medium and grown at 37°C with shaking until the OD_{600} was 0.6. Cells were then induced with 1 mmol L^{-1} isopropyl β-D-1-thiogalactopyranoside (IPTG) and cultured at 28°C for 12 h. Bacterial cells were centrifuged at 4,000 r min^{-1} for 20 min at 4°C, and the harvested cell pellets were used for protein purification.

For purification of GST fusion proteins, bacterial cells were suspended in phosphate buffered saline (PBS), lysed by sonication, and subjected to centrifugation at 8,000 r min^{-1} at 4°C for 20 min. Supernatants were then incubated with GST Sefinose™ Resin (Sangon, Shanghai, China) at 4°C for 1 h, and proteins were eluted with 10 mmol L^{-1} glutathione. For purification of His-tagged proteins, bacterial cells were suspended in cell lysis buffer (50 mmol L^{-1} NaH_2PO_4, 300 mmol L^{-1} NaCl pH 8, and 10 mmol L^{-1} imidazole), lysed by sonication, and subjected to centrifugation at 8,000 r min^{-1} at 4°C for 20 min. Supernatants were incubated with Ni-NTA Sefinose™ Resin 6FF (Sangon) at 4°C for 1 h, and proteins were then recovered with elution buffer (50 mmol L^{-1} NaH_2PO_4, 300 mmol L^{-1} NaCl, 250 mmol L^{-1} imidazole). Recombinant proteins were visualized on polyacrylamide gels stained with Coomassie brilliant blue.

2.12. Pull-down assays

Pull-down assays were performed as described previously (Zhai *et al.* 2019). GST Sefinose™ Resin was washed four times in PBS buffer and incubated with 6 μg purified GST-XopM or GST-XopL for 1 h; the resin was then collected, His-tagged OsAOS3 (6 μg) was added, and the mixture was incubated at 4°C for 2 h. Resins were then washed four times in PBS to remove non-specific bound proteins. Resins were harvested by centrifugation and then boiled in SDS buffer at 100°C for 10 min to release proteins. Next, proteins were separated on 10% SDS-PAGE gels (Genscript, Nanjing, China) and transferred to polyvinylidene difluoride (PVDF) membranes for immunoblotting with anti-GST or anti-His (TransGen Biotech, Beijing, China) as the primary antibody. The secondary antibody, goat anti-mouse immunoglobulin G (H+L) (TransGen Biotech, Beijing, China), was used to detect the primary antibody, and results were visualized using the LumiBest Western Kit (Share-Bio, Shanghai, China).

2.13. RNA extraction and qRT-PCR

Total RNAs of rice leaves challenged with *Xoo* at different time points were extracted with Trizol reagent (TaKaRa). cDNA was synthesized from total RNA (1 μg) using TransScript® One-Step gDNA Removal and cDNA Synthesis SuperMix (TransGen, Beijing, China). The qRT-PCR reactions were performed with TransStart® Tip Green qPCR SuperMix (+Dye II, TransGen) and the Applied Biosystems 7500 Real-Time PCR System (ThermoFisher, USA). *OsACTIN* was used as an internal control, and relative expression was calculated with the $2^{-\Delta\Delta Ct}$ method. qRT-PCR experiments were performed in triplicate.

2.14. Bimolecular fluorescence complementation (BiFC) assays

BiFC assays were conducted to detect possible interactions

between XopM and OsAOS3 in tobacco. The coding sequences of XopM and OsAOS3 were cloned into pSPYNE and pSPYCE, respectively. The recombinant constructs were transformed into *Agrobacterium* strain GV3101 and co-expressed in tobacco leaves using *Agrobacterium* infiltration. Fluorescence signals were detected using a confocal microscope (Leica TCS SP5 II) 48 h after infiltration.

2.15. Co-immunoprecipitation assay

XopM was cloned into the pC1300-GFP vector, and OsAOS3 was cloned into pCAMBIA-35S-cLuc with a LUC tag. The constructs were transformed into *Agrobacterium* GV3101 and co-expressed into tobacco. Fusion proteins were extracted in extraction buffer (50 mmol L^{-1} Tris-HCl, pH 7.5, 150 mmol L^{-1} NaCl, 5 mmol L^{-1} EDTA, 1% Triton X-100, 1 mmol L^{-1} DTT, 1 mmol L^{-1} PMSF). A total of 20 μL GFP Nanoab Mag Beads (Everylab, Shanghai) was added to each sample and incubated in 4°C for 1 h. Beads were washed with TBS buffer four times. The Magnetic beads were re-suspended using 2×SDS loading buffer and boiled in water for 10 min. Fusion proteins were detected by Western blot.

2.16. Measurement of JA

JA content was measured as described previously (Hui *et al.* 2023). Rice seedlings were collected from the greenhouse and macerated in liquid nitrogen. Samples were mixed with extraction buffer (methanol:acetic acid:water=80:1:19), incubated in darkness overnight at 4°C and centrifuged at 4°C for 20 min. The supernatant was transferred into a 1.5-mL microcentrifuge tube, dried under vacuum, and dissolved in 200 μL 30% methanol. JA was quantified with an AB SCIEX 4000Q TRAP LC/MS System (SCIEX QTRAP 5500).

3. Results

3.1. XopM contributes to the ETS induced by PthXo1 in rice

The relationship between TALEs and non-TALEs in the *Xoo*-rice interaction was explored by using the suicide vector pKMS1 to introduce the major TALE encoded by *pthXo1* into the *Xoo* strain PH (Ji *et al.* 2016) (Appendix B). *Xoo* PH is a *tal*-free strain of PXO99^{A} and harbors all non-TALE repertoires. We designed the knock-in construct pKMS1-PthXo1 to introduce *pthXo1* into its native site in the *Xoo* PH genome. After two-step exchanges and selection with kanamycin and sucrose, we obtained the knock-in strain named PH-PthXo1. The successful introduction of *pthXo1* into *Xoo* PH was evaluated by PCR, Southern blotting, and qRT-PCR (Appendix B). Several colonies were identified with the 976-bp PCR product corresponding to *pthXo1*, and sequence analysis confirmed that colonies contained *pthXo1*. Southern blots using *pthXo1* as a probe verified the successful introduction of this gene into *Xoo* PH. A previous study showed that the TALE effector PthXo1 upregulated the expression of *S* gene *OsSWEET11a* to promote disease development (Chen *et al.* 2010). Using qRT-PCR, we confirmed that the *Xoo* PH-PthXo1 strain induced *OsSWEET11a* expression in rice, whereas *Xoo* PH failed to induce expression (Appendix B). These findings indicated that *pthXo1* was functionally active in the *Xoo* PH-PthXo1 strain.

To evaluate the contribution of non-TALE effectors to virulence and their potential relationship with the major TALE PthXo1, we developed a screening technique to inactivate all 26 non-TALE genes present in *Xoo* PH. The genome of *Xoo* PXO99^{A}, the parental strain of *Xoo* PH, was used as a reference (http://www.biopred.net/xanthomonas/t3e.html). Twenty-six individual knockout mutants of non-TALEs in *Xoo* PH-PthXo1 were generated using pKMS1-mediated homologous recombination (Appendices D and E). The virulence of the 26 non-TALE mutants was evaluated in leaves of two-month-old Nipponbare and Kitaake rice. Pathogenicity tests showed that the XopM deletion mutant PH-PthXo1ΔM exhibited reduced virulence compared to *Xoo* PH-PthXo1 when inoculated to Nipponbare (Fig. 1) and Kitaake rice (Appendix F). The virulence of *Xoo* PH-PthXo1ΔM was restored to *Xoo* PH-PthXo1 levels by introducing *xopM in trans* (Fig. 1; Appendix F). These data indicate that *xopM* contributes to virulence and plays an important role in the ETS induced by the major TALE PthXo1. A remarkable reduction in the formation of water-soaked lesions was observed in leaves inoculated with *xopM* mutants, indicating that XopM may have other functions in pathogenicity (Appendix G).

XopM was initially identified as a T3SS effector in the phytopathogenic bacterium *Xcv*, and $xopM_{Xcv}$ was described as a 1,560-bp ORF that encodes 519 amino acids. BLASTP analysis (https://blast.ncbi.nlm.nih.gov) revealed the presence of a $XopM_{Xcv}$ homologue in PXO99^{A}, and this was designated $XopM_{Xoo}$. Sequence analysis indicated that $XopM_{Xoo}$ consists of 517 amino acids and shares 90.6% protein identity with $XopM_{Xcv}$, suggesting that $XopM_{Xoo}$ is a non-TALE protein secreted *via* the T3SS.

3.2. Subcellular localization of XopM in plant cells

The localization of XopM was analyzed by fusing green fluorescent protein (GFP) to $XopM_{Xoo}$ to form $XopM_{Xoo}$-GFP, which was transiently expressed in *N. benthamiana* leaves using agroinfiltration. The $XopM_{Xoo}$-GFP fusion accumulated in the tobacco cell membrane and cytoplasm (Fig. 2). Due to the fact that *xopM* from *Xoc* strain BLS256 (designated $xopM_{Xoc}$) shares 96.9% nucleotide similarity with $xopM_{Xoo}$ and encodes a protein of 517 amino acids, we also investigated the localization of $XopM_{Xoc}$ in tobacco. The $XopM_{Xoc}$-GFP fusion protein was also observed in the cell membrane and cytoplasm of *N. benthamiana* (Fig. 2). The GFP control localized to membrane, cytoplasm, and nucleus. In addition, we also studied the localization of XopM in rice protoplasts. GFP signals from $XopM_{Xoo}$-GFP and $XopM_{Xoc}$-GFP were detected in membranes, cytoplasm, and chloroplasts (Appendix H).

3.3. XopM interacts with allene oxide synthase OsAOS3

To understand how $XopM_{Xoo}$ interferes with the rice defense response, a yeast two-hybrid (Y2H) screen was conducted to identify proteins that interact with $XopM_{Xoo}$ using a cDNA

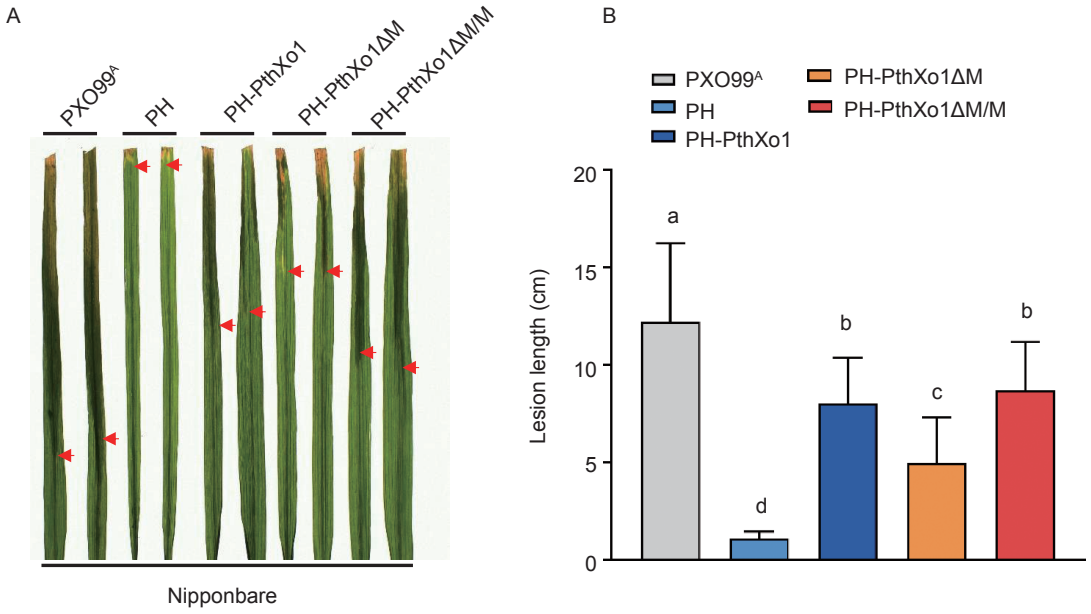


Fig. 1 Pathogenicity assay of *Xanthomonas oryzae* pv. *oryzae* (*Xoo*) *xopM* mutants in rice. A, virulence assays in rice cultivar Nipponbare. Field-grown, two-month-old rice plants were inoculated with *Xoo* PXO99^{A}, PH, and mutants using the leaf-clipping method. *Xoo* PXO99^{A} is a wild-type strain that harbors both TALE and non-TALE effectors; PH is a *tal*-free strain; PH-PthXo1 contains an introduced copy of the TALE *pthXo1*; PH-PthXo1ΔM is a *xopM* mutant of *Xoo* strain PH-PthXo1; and PH-PthXo1ΔM/M represents PH-PthXo1ΔM complemented with *xopM in trans*. Photographs were taken 14 d after inoculation. The red arrows indicate the extent of lesion expansion. B, lesion lengths produced by *Xoo* in rice cv. Nipponbare. Lesions were measured 14 d after inoculation with *Xoo*. Each value is the mean±SD. Data were analyzed for significance using one-way ANOVA with Tukey's test (P≤0.05). Columns labeled with different letters indicate statistically significant differences. Each experiment was performed three times with similar results.

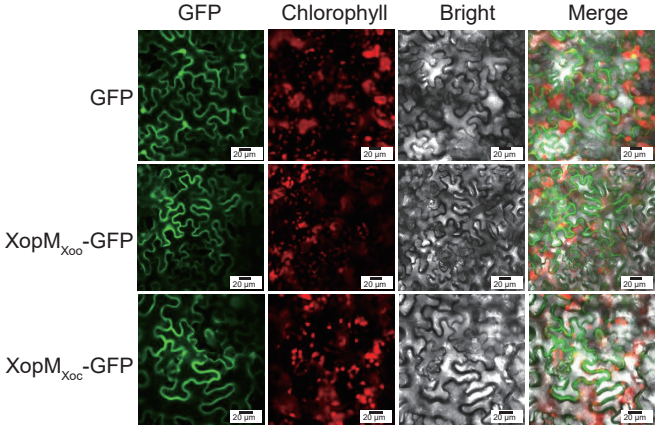


Fig. 2 Localization of XopM in plant cells. Subcellular localization of XopM$_{Xoo}$-GFP, XopM$_{Xoc}$-GFP and GFP in tobacco. The coding sequences of *xopM*$_{Xoo}$ and *xopM*$_{Xoc}$ were cloned into *Kpn*I/*Xba*I-digested pC1300-GFP and introduced into *Agrobacterium* GV3101 for transient expression in tobacco. Autofluorescence of chlorophyll is depicted in red. The brightfield and merged images are shown in the third and fourth columns, respectively. Scale bars, 20 μm. The experiment was repeated three times with similar results.

library generated from rice infected with *Xoo* PXO99^{A}. Full-length *xopM* in pGBKT7 was used as bait to screen the rice cDNA library. An allene oxide synthase encoded by *Os02g0218700* (*OsAOS3*) was found to interact with XopM (Appendix I). *OsAOS3* is a 1.5-kb ORF without introns and encodes a key enzyme in the JA biosynthetic pathway (Haga and Iino 2004). To further confirm the interaction, we cloned the coding sequence of *OsAOS3* into pGADT7 and co-transformed the constructs into *Saccharomyces cerevisiae* AH109 with pGBKT7-XopM. The transformants were inoculated to SD/–Leu–Trp–His–Ade selective medium with X-α-gal. The Y2H experiments confirmed that XopM$_{Xoo}$ interacted with OsAOS3 (Fig. 3-A).

To further confirm the physical interaction of XopM$_{Xoo}$ and OsAOS3, we performed split luciferase complementation (SLC) and pull-down assays. The coding sequences of *xopM*$_{Xoo}$ and *xopM*$_{Xoc}$ were inserted into pCAMBIA-35S-nLuc (nLuc), and *OsAOS3* was cloned in pCAMBIA-35S-cLuc (cLuc); these constructs were then transformed into *Agrobacterium* GV3101 and infiltrated into tobacco leaves. Fluorescent signals were detected 48 h after inoculation and indicated an interaction between XopM$_{Xoo}$ and OsAOS3 (Fig. 3-B). Fluorescent signals were absent when nLuc/cLuc-OsAOS3 and XopM$_{Xoo}$-nLuc/cLuc were co-expressed (Fig. 3-B). Sequence analysis showed that the four AOS proteins (OsAOS1, OsAOS2, OsAOS3, and OsAOS4) in rice contained conserved I-helices and heme-binding domains (Haga and Iino 2004). Domain deletion analysis showed that OsAOS3 lacking I-helices and heme-binding domains did not abolish the interaction with XopM but instead reduced protein affinity (Appendix J). Furthermore, a direct physical interaction between glutathione *S*-transferase (GST)-XopM and His-OsAOS3 was confirmed in pull-down assays (Fig. 3-C). To determine the localization of their interaction, we performed bimolecular fluorescence complementation

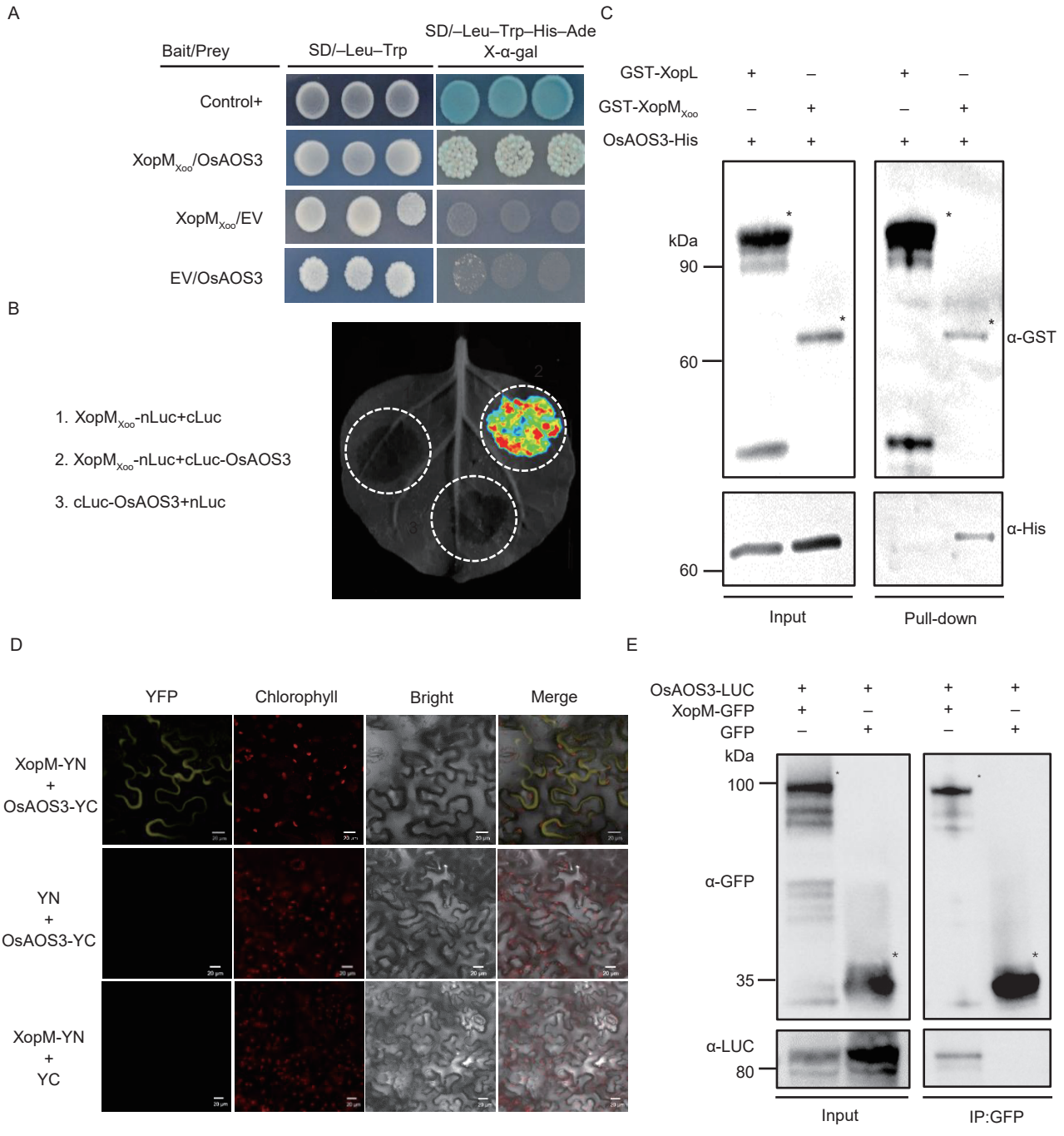


Fig. 3 XopM interacts with allene oxide synthase OsAOS3. A, yeast two-hybrid assay showing interactions between XopM and OsAOS3. *xopM* was cloned into *Eco*RI/*Sal*I-digested pGBKT7 to form the bait construct pGBKT7-XopM, and *OsAOS3* was cloned into *EcoR*I/*Bam*HI-digested pGADT7 to form the prey construct pGADT7-OsAOS3. Interactions between XopM and OsAOS3 were screened on SD/–Leu–Trp–His–Ade agar medium with 20 mg mL^{-1} X-α-GAL. Constructs pGBKT7-53 and pGADT7-T were co-transformed into yeast cells and used as positive controls. EV indicates empty vector, and experiments were repeated three times. B, split luciferase complementation (SLC) assay of XopM$_{Xoo}$-nLuc and cLuc-OsAOS3 interactions in *Nicotiana benthamiana*. The coding sequences of *xopM*$_{Xoo}$ and *OsAOS3* were PCR-amplified and cloned into pCAMBIA-35S-nLuc and pCAMBIA-35S-cLuc, respectively. The constructs were transformed into *Agrobacterium* GV3101, cultured overnight with selection, induced, and then infiltrated into tobacco leaves. Luciferase activity was measured at 48 h post-inoculation (hpi). C, *in vitro* interactions between XopM and OsAOS3. Purified GST-XopL (negative control) and GST-XopM proteins were incubated with OsAOS3-His, and glutathione-Sepharose 4B beads were added to evaluate protein–protein interactions. Anti-GST or anti-His antibodies were used to detect fusion proteins, and GST-XopL was used as a negative control. Two separate experiments produced similar results. Molecular weight marker bands (kDa) are indicated for reference. D, bimolecular fluorescence complementation (BiFC) assay of YN-tagged XopM with YC-tagged OsAOS3 in *Agrobacterium*-infiltrated *N. benthamiana* leaves. The YC and YN vector contain the C- and N-terminal halves of yellow fluorescent protein, respectively. The first column indicates the interaction of YN- with YC-labeled proteins. The second column shows the autofluorescence of chlorophyll in red; the third and fourth columns show the brightfield and merged images, respectively. Scale bars, 20 μm. E, XopM interacts with OsAOS3 in CoIP assay. Fusion proteins extracted from tobacco leaves and immunodetected using GFP and LUC antibody. * indicates the target protein.

(BiFC) assays, and the results showed that XopM and OsAOS3 interact predominantly in the plasma membrane (Fig. 3-D). A coimmunoprecipitation (CoIP) assay confirmed that XopM interacts with OsAOS3 *in planta* (Fig. 3-E). Collectively, these data demonstrate that XopM interacts with OsAOS3 both *in vitro* and *in planta*.

The rice genome contains four *OsAOS* genes (*OsAOS1*, *OsAOS2*, *OsAOS3*, and *OsAOS4*) with roles in the biosynthesis of the JA precursor 12-oxo-phytodienoic acid (OPDA) (Haga and Iino 2004). In addition to the interaction with OsAOS3, we found that $XopM_{Xoo}$ also interacted with OsAOS1, OsAOS2, and OsAOS4, respectively (Appendix K), suggesting that the interaction with $XopM_{Xoo}$ is conserved in the OsAOS family in rice.

$XopM_{Xoc}$ shares a high level of sequence homology with $XopM_{Xoo}$ (93.8% amino acid identity); consequently, we hypothesized that $XopM_{Xoc}$ can interact with OsAOS3. The interaction was verified in SLC assays using $XopM_{Xoc}$-nLuc and cLuc-OsAOS3 and was further confirmed in western blots (Appendix L). The other three homologous proteins also interacted with $XopM_{Xoc}$, which confirms that $XopM_{Xoc}$ also interacts with OsAOSs.

3.4. *OsAOS* genes are activated during *Xoo* infection in rice

To examine *OsAOS* expression in response to *Xoo* infection, we evaluated the expression of all four *OsAOS* genes in rice challenged with the *Xoo* strain PXO99^A. The relative expression of all four *OsAOS* genes increased at 2 h after inoculation and then rapidly decreased to a basal level (Fig. 4-A). The expression of *OsAOS* genes after inoculation with *Xoo* PXO99^A indicated that these genes respond to infection at an early stage and are likely involved in the defense response. To further determine the function of OsAOS3 in plant cells, we performed localization studies in tobacco leaves. The *OsAOS3* coding sequence was fused with a GFP construct driven by the CaMV 35S promoter and introduced into *N. benthamiana* for localization assays. The GFP signal was observed in chloroplasts (Fig. 4-B), indicating that *OsAOS3* functions in this organelle.

3.5. OsAOS3 positively regulates rice immunity

To investigate whether *OsAOS3* confers resistance to bacterial disease in rice, we generated *OsAOS3* knockout mutants using CRISPR/Cas9-mediated gene editing to disrupt the coding sequence of *OsAOS3*. A total of 26 OsAOS3 transgenic lines were obtained. Fourteen heterozygotes and eight homozygotes were detected by PCR and confirmed by sequencing (Appendix M). Two homozygotes from the T1 generation (*CRI-OsAOS3-8* and *CRI-OsAOS3-18*) were chosen for further study (Appendix N). The two *osaos3* mutant lines exhibited increased susceptibility to *Xoo* PXO99^A and *Xoc* BLS256 infection as compared to Nipponbare (Fig. 5-A and B). To test whether JA-mediated immunity was impaired in *osaos3* mutants, the expression of two JA pathway-related defense genes was determined. The results showed that *OsPBZ1* and *OsWRKY13* were downregulated in *osaos3* mutants after *Xoo* treatment, suggesting the potential role of OsAOS3 in resistance (Fig. 5-C and D). JA levels were also measured in wild-type Nipponbare and *osaos3* mutants both with and without *Xoo* inoculation, and the results showed that JA accumulation was reduced in *osaos3* mutants as compared to Nipponbare (Fig. 5-E; Appendix O). Furthermore, the expression level of the JA responsive gene *OsJAZ8* was measured after inoculation with *Xoo* PXO99^A. Expression of *OsJAZ8* was downregulated in the *osaos3* mutants at 6 hpi (Fig. 5-F). These results indicate that *OsAOS3* plays a role in JA biosynthesis and contributes to defense.

3.6. XopM interferes with JA-mediated plant defense

Emerging evidence has revealed an important role for JA in the host response to pathogen infection (Hui *et al.* 2019;

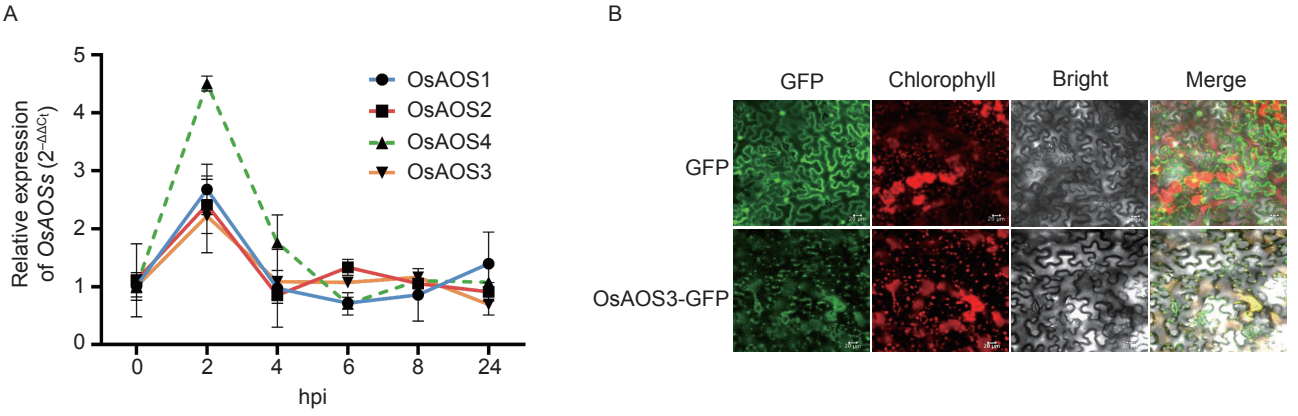


Fig. 4 *OsAOS* genes are involved in the response to *Xanthomonas oryzae* pv. *oryzae* (*Xoo*) infection. A, relative expression of *OsAOS1*, *OsAOS2*, *OsAOS3*, and *OsAOS4* during *Xoo* infection. Expression levels were determined by qRT-PCR after inoculation with *Xoo* PXO99^A at 2, 4, 6, 8, and 24 h post-inoculation (hpi); inoculation with water served as a control, and *OsACTIN* was chosen as a reference gene. Relative expression was calculated with the $2^{-\Delta\Delta Ct}$ method, and each value represents the mean±SE (n=3). The experiment was repeated three times with similar results. B, the subcellular location of OsAOS3-GFP and the GFP control in transfected tobacco. Autofluorescence of chlorophyll is depicted in red, and the brightfield and merged images are shown in the third and fourth columns, respectively. The results were repeated three times with similar results.

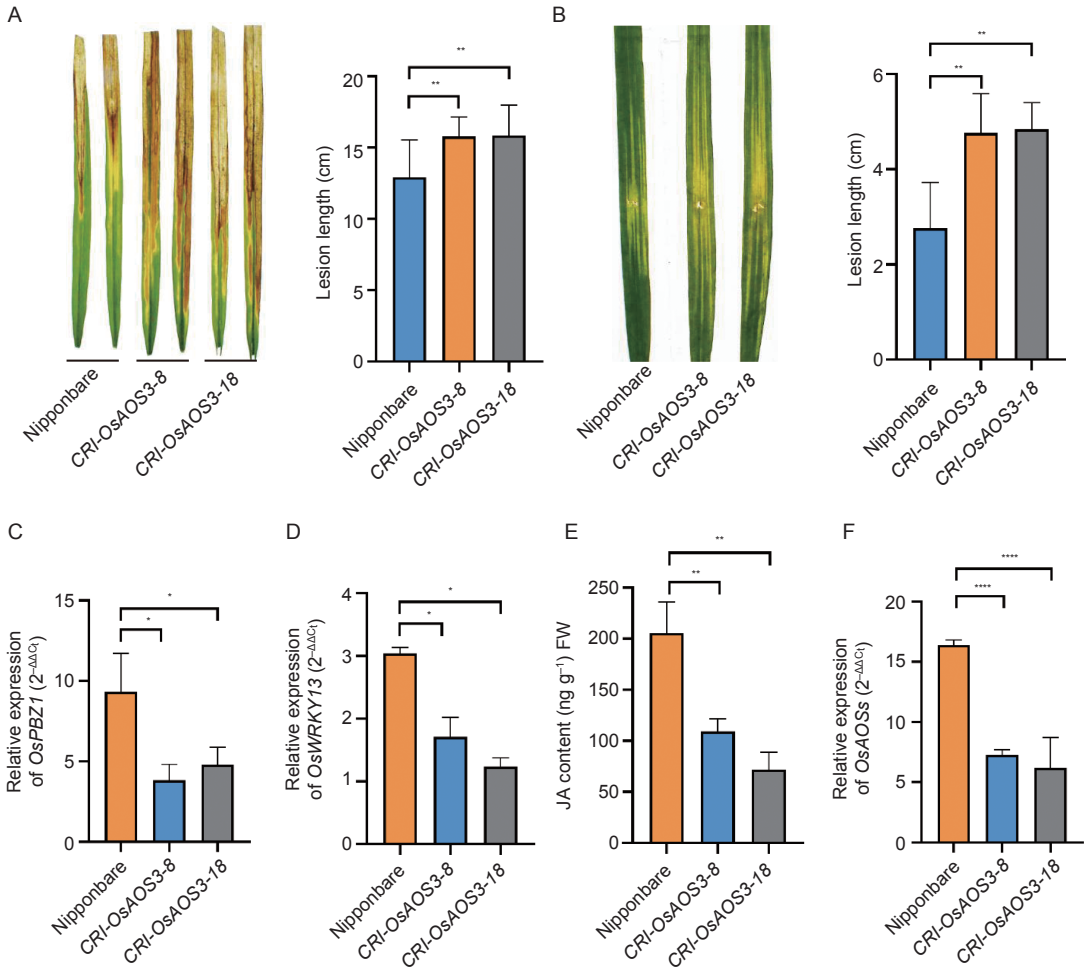


Fig. 5 OsAOS3 contributes to the rice immune response. A and B, disease phenotypes and lesions lengths on Nipponbare and *osaos3* mutants inoculated with *Xoo* PXO99^{A} and *Xoc* BLS256. Leaves were collected and photographed at 14 and 7 d after *Xoo* and *Xoc* inoculation, respectively. C and D, relative expression of JA pathway-related genes, *OsPBZ1* and *OsWRKY13*. Rice leaves were infiltrated with *Xoo* PXO99^{A} (OD_{600}=0.8) or mock-inoculated with sterile water (control), and leaf samples were collected 6 h post-inoculation (hpi). E, JA content in *Xoo*-infiltrated rice leaves. Leaves of Nipponbare and *osaos3* mutant rice lines were infiltrated with *Xoo* PXO99^{A}. Leaves were collected at 4 hpi, and JA was measured by LC/MS. F, relative expression of the JA responsive gene *OsJAZ8*. The housekeeping gene *OsACTIN* was used as a reference gene. Data represent the mean±SD (A) and mean±SE (B–F) of three biological replicates, and asterisks indicate significant differences (Student's *t*-test, *, P<0.05; **, P<0.01; ****, P<0.0001). Three independent experiments were performed in triplicate.

Ruan *et al.* 2019). To explore whether XopM affects JA biosynthesis by interacting with OsAOS3, we measured the JA content in Nipoonbare after challenge with *Xoo* PXO99^{A}, PH-PthXo1, PH-PthXo1ΔM and PH-PthXo1ΔM/M. The JA level of rice challenged by *Xoo* PH-PthXo1ΔM was significantly higher than levels observed in *Xoo* PH-PthXo1 and PH-PthXo1ΔM/M inoculated lines (Fig. 6-A). To investigate whether XopM affects JA-mediated immunity, we performed qRT-qPCR analysis of the mRNA from rice leaves infiltrate with PXO99^{A}, PH-PthXo1, PH-PthXo1ΔM, PH-PthXo1ΔM/M. The JA-related immune genes, *OsJAZ8*, *OsPBZ1*, *OsWRKY13*, *OsPR1*, and *OsPAL* were transcriptionally repressed in *Xoo* PH-PthXo1 and PH-PthXo1ΔM/M-infiltrated leaves as compared to expression levels in rice inoculated with the *xopM* mutants (Fig. 6-B–F). Collectively, the results indicate that XopM decreases JA signal transduction resulting in suppression of the defense response.

4. Discussion

The arms race between plants and pathogens is complicated due to overlapping effector proteins and the complex layers of plant immunity (Guttman *et al.* 2002; Hillmer *et al.* 2017; Tyler 2017); consequently, it is critical to identify effector target proteins in the plant cell. This study shows that an enzyme in JA biosynthesis, OsAOS3, contributes to plant defense and is hijacked by the conserved effector XopM, which suppresses JA-mediated immunity. XopM interacts with the allene oxide synthase OsAOS3 *in planta* and *in vitro*. Our results indicate that *Xoo* deploys XopM and physically interacts with OsAOS3, resulting in compromised JA-related defense responses and subsequent disease development (Fig. 7).

Xanthomonas delivers more than 30 effectors into plant cells, including the Xop proteins that subvert host defense responses. However, it is difficult to study the contribution of individual Xop proteins to virulence because of Xop

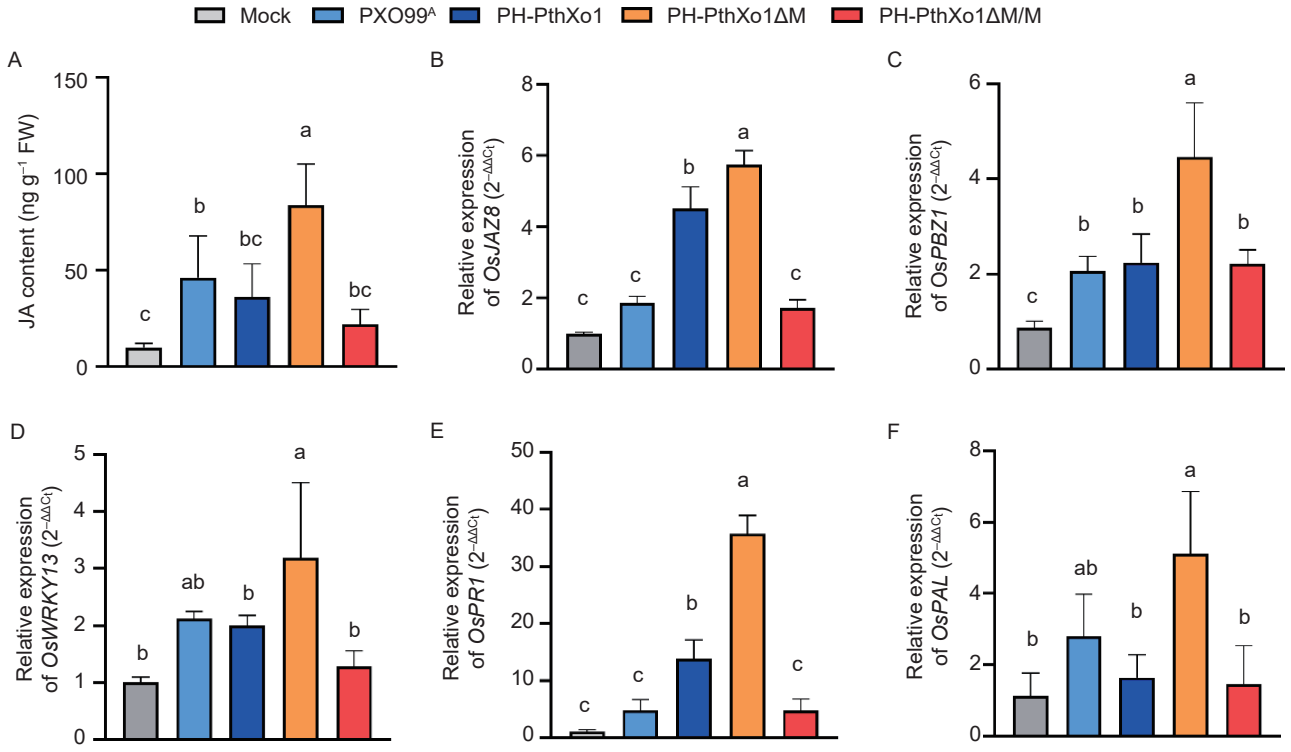


Fig. 6 XopM interferes with the *Xoo*-elicited JA-mediated plant defense response. A, comparison of JA levels in Nipponbare infiltrated with sterile water (mock-inoculated), *Xoo* PXO99^{A}, PH-PthXo1, PH-PthXo1ΔM, and PH-PthXo1ΔM/M. Columns labeled with different letters indicate statistically significant differences. B–F, expression of downstream JA immune-response genes *OsJAZ8*, *OsPBZ1*, *OsWRKY13*, *OsPR1*, and *OsPAL* in Nipponbare rice infiltrated with sterile water (mock), *Xoo* PXO99^{A}, PH-PthXo1, PH-PthXo1ΔM, and PH-PthXo1ΔM/M. Each value represents the mean±SE. Data were analyzed by one-way ANOVA (Tukey's test, $P<0.05$). Columns labeled with different letters indicate statistically significant differences. Each experiment was performed three times with similar results.

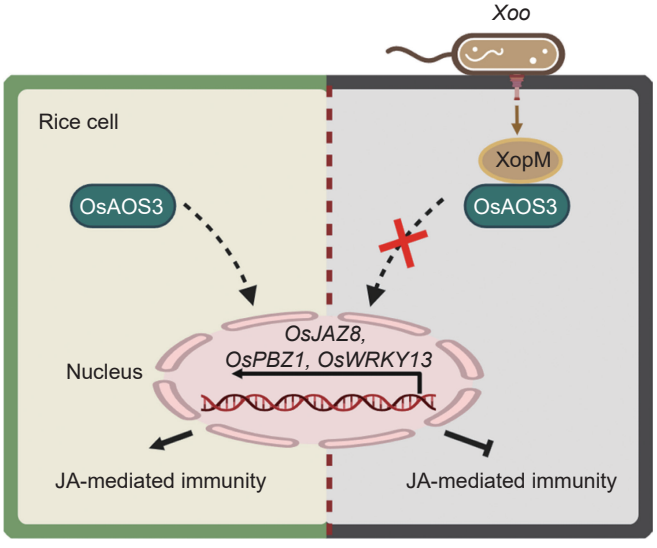


Fig. 7 Model showing how XopM interferes with JA-mediated immunity in rice. In this paradigm, rice cells perceive conserved pathogen-associated molecular patterns associated with *Xoo* and trigger JA-mediated defense responses. This leads to enhanced expression of defense genes (*OsJAZ8*, *OsPBZ1*, and *OsWRKY13*) and increased resistance to bacterial blight of rice. *Xoo* subverts JA mediate defense response *via* the effector XopM, which targets allene oxide synthase OsAOS3. As a result, the expression of downstream defense genes (*OsJAZ8*, *OsPBZ1*, and *OsWRKY13*) is reduced, resulting in disease development in rice.

redundancy and the presence of TALEs (Song and Yang 2010; Sinha *et al.* 2013). In previous studies, *Xoo* PH, a *tal*-free derivative of PXO99^{A}, was used to probe the function of TALEs from *Xanthomonas* spp. on susceptible and resistant rice cultivars (Ji *et al.* 2016; Xu *et al.* 2019). Here, we establish a system to evaluate the effect of a single non-TALE on virulence, and our approach eliminates possible interference by redundant TALEs.

In this study, we found that XopM plays an important role in virulence. It is worth noting that XopM is highly conserved in sequenced *Xanthomonas* genomes (Merda *et al.* 2017). Both genomic and transcriptomic analyses identified XopM as a core effector involved in overcoming basal immunity (Roux *et al.* 2015; Merda *et al.* 2017). It was previously identified as a secreted protein with characteristics of non-TALE effectors, and experiments conducted *in planta* showed that *xopM* was co-expressed with T3SS genes (Schulze *et al.* 2012). XopM has been shown to inhibit MAPK-mediated cell death in *N. benthamiana* (Teper *et al.* 2015). Collectively, these findings indicate that XopM is a conserved effector involved in the suppression of host immunity. Our results showed that XopM interacted directly with OsAOS3 *in planta* and *in vitro* (Fig. 3). The interaction observed predominantly in the cell membrane indicates that XopM might hijack OsAOS3 to subvert its function by interfering with its localization to chloroplasts, which requires further study. Inspection of the deduced protein sequence of XopM$_{Xoo}$ failed to reveal

functional domains, so it remains unclear what portion of XopM interacts with OsAOS3.

Allene oxide synthases belong to the P450 family and catalyze the production of 12,13-epoxy-octadecatrienoic acid (allene oxide), which is the first intermediate in the JA pathway (Kuroda *et al.* 2005). Our results show that all four *OsAOS* genes can respond to *Xoo* infection, which indicates that these four genes may be involved in the plant-pathogen interaction. Among these, *osaos3* mutants exhibit a defect in JA biosynthesis compared to wild type, which indicates OsAOS3 plays an important role in JA biosynthesis and host resistance to *Xoo* and *Xoc*. However, the role of other *OsAOS* genes in JA synthesis and disease resistance cannot be ignored. For example, *OsAOS2* has been reported to participate in JA biosynthesis and resistance to rice blast and bacterial leaf blight (Hui *et al.* 2023; Wang *et al.* 2023; You *et al.* 2023). Some research studies have shown that *OsAOS2* functions in plant immunity; for example, *OsAOS2* expression was induced by *Xoo* and positively regulated plant immunity (Hui *et al.* 2023). *OsAOS2* expression peaked at 2 h after infection and then decreased to normal levels (Hui *et al.* 2023), which is consistent with our findings (Fig. 4-A). In addition, we found that the JA content with *Xoo* infection is higher than without infection in *osaos3* mutants (Fig. 5-E; Appendix O), which indicates that the other three OsAOSs may also be involved in JA biosynthesis in response to *Xoo* infection. These results suggest that OsAOS3 plays an important role in JA biosynthesis, while other *OsAOS* genes may play similar roles in JA biosynthesis and resistance, which may indicate a path forward for molecular plant breeding programs.

Our work provides novel insights into JA-associated disease development. We have identified a pathogen effector protein that targets a phytohormone enzyme, and the outcome is impaired plant immunity. There is mounting evidence in support of phytohormone signaling pathways in plant defense against pathogens (Robert-Seilaniantz *et al.* 2011; Ding and Ding 2020; Kim *et al.* 2022). The JA pathway is activated rapidly upon insect or pathogen attack, and a speedy response is imperative for immunity. Induced defense responses are closely associated with JA when plants are under attack by necrotrophic pathogens; for example, JA co-receptor CORONATINE INSENSITIVE 1 (Coi1-1) mutants show increased susceptibility to necrotrophic fungi (Thomma *et al.* 1998; Yan and Xie 2015). Moreover, recent evidence has shown that the JA signaling pathway also plays an important role in plant resistance against bacteria. Overexpression of the JA biosynthesis-related gene *OsAOS1* conferred an elevated level of resistance to *Xoo*, which supports the role of the JA pathway in plant immune responses (Hou *et al.* 2019). Consistent with this, our findings show that *OsAOS3* mutants exhibited lower levels of endogenous JA and decreased resistance to *Xoo* and *Xoc* (Fig. 5-A, B, and E), suggesting that the JA-mediated defense is effective against more than one bacterial pathogen. As a counter measure, pathogens have evolved a variety of effectors that subvert host cell physiology and promote disease development by hijacking plant hormone components, and examples include the effectors XopC2 and HopX1 from *X. oryzae* and *Pseudomonas syringae*, respectively (Gimenez-Ibanez *et al.* 2014; Peng *et al.* 2019; Wang *et al.* 2021). This strategy also applies to virus-plant interactions; for example, the nonstructural proteins encoded by tomato spotted wilt orthotospovirus target the repressor TCP21 to decrease the function of phytohormone receptors, thereby promoting virulence (Chen *et al.* 2023). Similarly, our results indicate that the introduction of XopM into the plant cell impairs JA-mediated defense by interacting with OsAOS3 (Fig. 7). Collectively, these findings suggest that *Xanthomonas* employs multiple effectors to attack several targets in JA signaling pathways as a way to thwart the host immune system. Since extensive crosstalk exists among phytohormone pathways, it remains possible that SA and/or ET pathways are affected by disturbed JA-mediated defenses.

5. Conclusion

This study highlights a novel virulence strategy for pathogenesis where XopM targets the JA biosynthetic enzymes OsAOS3. Our results show that *Xoo* impedes JA-mediated disease resistance in rice *via* XopM. The findings described in this study further our understanding of the virulence mechanisms utilized by bacterial pathogens, which may be helpful in the context of improved disease control.

Acknowledgements

The authors thank Dr. Bing Yang (University of Missouri, USA) for providing the plasmids needed for the CRISPR/Cas9 system. This work was supported by the National Natural Science Foundation of China (31830072 and 32102147).

Declaration of competing interest

The authors declare no competing financial interests.

Declaration of generative AI and AI-assisted technologies in the writing process

The authors declare that they did not use AI in the preparation and writing of this manuscript.

Appendices associated with this paper are available at https://doi.org/10.1016/j.jia.2024.08.018

References

Bittner A, Cieśla A, Gruden K, Lukan T, Mahmud S, Teige M, Vothknecht U C, Wurzinger B. 2022. Organelles and phytohormones: A network of interactions in plant stress responses. *Journal of Experimental Botany*, **73**, 7165–7181.

Boller T, He S Y. 2009. Innate immunity in plants: An arms race between pattern recognition receptors in plants and effectors in microbial pathogens. *Science*, **324**, 742–744.

Campos M L, Kang J H, Howe G A. 2014. Jasmonate-triggered plant immunity. *Journal of Chemical Ecology*, **40**, 657–675.

Chen J, Zhao Y, Luo X, Hong H, Yang T, Huang S, Wang C, Chen H, Qian X, Feng M, Chen Z, Dong Y, Ma Z, Li J, Zhu M, He S Y, Dinesh-Kumar S P, Tao X. 2023. NLR surveillance of pathogen interference with hormone receptors induces immunity. *Nature*, **613**, 145–152.

Chen L Q, Hou B H, Lalonde S, Takanaga H, Hartung M L, Qu X Q, Guo W J, Kim J G, Underwood W, Chaudhuri B, Chermak D, Antony G, White F F, Somerville S C, Mudgett M B, Frommer W B. 2010. Sugar

transporters for intercellular exchange and nutrition of pathogens. *Nature*, **468**, 527–532.
Deb S, Ghosh P, Patel H K, Sonti R V. 2020. Interaction of the *Xanthomonas* effectors XopQ and XopX results in induction of rice immune responses. *The Plant Journal*, **104**, 332–350.
Deslandes L, Rivas S. 2012. Catch me if you can: Bacterial effectors and plant targets. *Trends in Plant Science*, **17**, 644–655.
Ding P T, Ding Y L. 2020. Stories of salicylic acid: A plant defense hormone. *Trends in Plant Science*, **25**, 549–565.
Dodds P N, Rathjen J P. 2010. Plant immunity: Towards an integrated view of plant-pathogen interactions. *Nature Reviews Genetics*, **11**, 539–548.
Dou D L, Zhou J M. 2012. Phytopathogen effectors subverting host immunity: Different foes, similar battleground. *Cell Host Microbe*, **12**, 484–495.
Furutani A, Takaoka M, Sanada H, Noguchi Y, Oku T, Tsuno K, Ochiai H, Tsuge S. 2009. Identification of novel type III secretion effectors in *Xanthomonas oryzae* pv. *oryzae*. *Molecular Plant-Microbe Interactions*, **22**, 96–106.
Gimenez-Ibanez S, Boter M, Fernández-Barbero G, Chini A, Rathjen J P, Solano R. 2014. The bacterial effector HopX1 targets JAZ transcriptional repressors to activate jasmonate signaling and promote infection in *Arabidopsis*. *PLoS Biology*, **12**, e1001792.
Gomi K, Satoh M, Ozawa R, Shinonaga Y, Sanada S, Sasaki K, Matsumura M, Ohashi Y, Kanno H, Akimitsu K, Takabayashi J. 2010. Role of hydroperoxide lyase in white-backed planthopper (*Sogatella furcifera* Horváth)-induced resistance to bacterial blight in rice, *Oryza sativa* L. *The Plant Journal*, **61**, 46–57.
Guttman D S, Vinatzer B A, Sarkar S F, Ranall M V, Kettler G, Greenberg J T. 2002. A functional screen for the type III (Hrp) secretome of the plant pathogen *Pseudomonas syringae*. *Science*, **295**, 1722–1726.
Haga K, Iino M. 2004. Phytochrome-mediated transcriptional up-regulation of ALLENE OXIDE SYNTHASE in rice seedlings. *Plant and Cell Physiology*, **45**, 119–128.
Hillmer R A, Tsuda K, Rallapalli G, Asai S, Truman W, Papke M D, Sakakibara H, Jones J D G, Myers C L, Katagiri F. 2017. The highly buffered *Arabidopsis* immune signaling network conceals the functions of its components. *PLoS Genetics*, **13**, e1006639.
Hou Y X, Wang Y F, Tang L Q, Tong X H, Wang L, Liu L M, Huang S W, Zhang J. 2019. SAPK10-mediated phosphorylation on WRKY72 releases its suppression on jasmonic acid biosynthesis and bacterial blight resistance. *iScience*, **16**, 499–510.
Hu Y Z, Ding Y X, Cai B Y, Qin X H, Wu J N, Yuan M H, Wan S W, Zhao Y, Xin X F. 2022. Bacterial effectors manipulate plant abscisic acid signaling for creation of an aqueous apoplast. *Cell Host Microbe*, **30**, 518–529.
Hui S G, Hao M Y, Liu H B, Xiao J H, Li X H, Yuan M, Wang S P. 2019. The group I GH3 family genes encoding JA-Ile synthetase act as positive regulator in the resistance of rice to *Xanthomonas oryzae* pv. *oryzae*. *Biochemical and Biophysical Research Communications*, **508**, 1062–1066.
Hui S G, Ke Y G, Chen D, Wang L, Li Q Q, Yuan M. 2023. Rice microRNA156/529-SQUAMOSA PROMOTER BINDING PROTEIN-LIKE7/14/17 modules regulate defenses against bacteria. *Plant Physiology*, **192**, 2537–2553.
Ji H T, Liu D L, Zhang Z X, Sun J W, Han B, Li Z Y. 2020. A bacterial F-box effector suppresses SAR immunity through mediating the proteasomal degradation of OsTrxh2 in rice. *The Plant Journal*, **104**, 1054–1072.
Ji Z Y, Ji C H, Liu B, Zou L F, Chen G Y, Yang B. 2016. Interfering TAL effectors of *Xanthomonas oryzae* neutralize R-gene-mediated plant disease resistance. *Nature Communications*, **7**, 13435.
Jones J D, Dangl J L. 2006. The plant immune system. *Nature*, **444**, 323–329.
Kim J H, Castroverde C D M, Huang S, Li C, Hilleary R, Seroka A, Sohrabi R, Medina-Yerena D, Huot B, Wang J, Nomura K, Marr S K, Wildermuth M C, Chen T, MacMicking J D, He S Y. 2022. Increasing the resilience of plant immunity to a warming climate. *Nature*, **607**, 339–344.
Kokkirala V R, Yonggang P, Abbagani S, Zhu Z, Umate P. 2010. Subcellular localization of proteins of *Oryza sativa* L. in the model tobacco and tomato plants. *Plant Signaling and Behavior*, **5**, 1336–1341.
Kuroda H, Oshima T, Kaneda H, Takashio M. 2005. Identification and functional analyses of two cDNAs that encode fatty acid 9-/13-hydroperoxide lyase (CYP74C) in rice. *Bioscience, Biotechnology and Biochemistry*, **69**, 1545–1554.
Li C, Xu M, Cai X, Han Z G, Si J P, Chen D H. 2022. Jasmonate signaling pathway modulates plant defense, growth, and their trade-offs. *International Journal of Molecular Sciences*, **23**, 3945.
Li Y R, Zou H S, Che Y Z, Cui Y P, Guo W, Zou L F, Chatterjee S, Biddle E M, Yang C H, Chen G Y. 2011. A novel regulatory role of HrpD6 in regulating *hrp-hrc-hpa* genes in *Xanthomonas oryzae* pv. *oryzicola*. *Molecular Plant-Microbe Interactions*, **24**, 1086–1101.
Lin J S, Lai E M. 2017. Protein-Protein interactions: Yeast Two-hybrid system. *Methods in Molecular Biology*, **1615**, 177–187.
Long J Y, Song C F, Yan F, Zhou J H, Zhou H B, Yang B. 2018. Non-TAL effectors from *Xanthomonas oryzae* pv. *oryzae* suppress peptidoglycan-triggered MAPK activation in rice. *Frontiers in Plant Science*, **9**, 1857.
Major I T, Yoshida Y, Campos M L, Kapali G, Xin X F, Sugimoto K, de Oliveira Ferreira D, He S Y, Howe G A. 2017. Regulation of growth-defense balance by the JASMONATE ZIM-DOMAIN (JAZ)-MYC transcriptional module. *New Phytologist*, **215**, 1533–1547.
Mei C S, Qi M, Sheng G Y, Yang Y N. 2006. Inducible overexpression of a rice allene oxide synthase gene increases the endogenous jasmonic acid level, *PR* gene expression, and host resistance to fungal infection. *Molecular Plant-Microbe Interactions*, **19**, 1127–1137.
Meng F W, Yang C, Cao J D, Chen H, Pang J H, Zhao Q Q, Wang Z Y, Fu Z Q, Liu J. 2020. A bHLH transcription activator regulates defense signaling by nucleo-cytosolic trafficking in rice. *Journal of Integrative Plant Biology*, **62**, 1552–1573.
Merda D, Briand M, Bosis E, Rousseau C, Portier P, Barret M, Jacques M A, Fischer-Le Saux M. 2017. Ancestral acquisitions, gene flow and multiple evolutionary trajectories of the type three secretion system and effectors in *Xanthomonas* plant pathogens. *Molecular Ecology*, **26**, 5939–5952.
Ngou B P M, Jones J D G, Ding P. 2022. Plant immune networks. *Trends in Plant Science*, **27**, 255–273.
Pan X Y, Xu S, Wu J, Duan Y B, Zheng Z T, Wang J X, Song X S, Zhou M G. 2018. Ankyrin-like protein AnkB interacts with CatB, affects catalase activity, and enhances resistance of *Xanthomonas oryzae* pv. *oryzae* and *Xanthomonas oryzae* pv. *oryzicola* to phenazine-1-carboxylic acid. *Applied and Environmental Microbiology*, **84**, e02145–17.
Peng Z, Hu Y, Zhang J, Huguet-Tapia J C, Block A K, Park S, Sapkota S, Liu Z H, Liu S Z, White F F. 2019. *Xanthomonas translucens* commandeers the host rate-limiting step in ABA biosynthesis for disease susceptibility. *Proceedings of the National Academy of Sciences of the United States of America*, **116**, 20938–20946.
Pieterse C M, Van der Does D, Zamioudis C, Leon-Reyes A, Van Wees S C. 2012. Hormonal modulation of plant immunity. *Annual Review of Cell and Developmental Biology*, **28**, 489–521.
Robert-Seilaniantz A, Grant M, Jones J D. 2011. Hormone crosstalk in plant disease and defense: More than just jasmonate-salicylate antagonism. *Annual Review of Phytopathology*, **49**, 317–343.
Roussin-Léveillée C, Lajeunesse G, St-Amand M, Veerapen V P, Silva-Martins G, Nomura K, Brassard S, Bolaji A, He S Y, Moffett P. 2022. Evolutionarily conserved bacterial effectors hijack abscisic acid signaling to induce an aqueous environment in the apoplast. *Cell Host Microbe*, **30**, 489–501.
Roux B, Bolot S, Guy E, Denancé N, Lautier M, Jardinaud M F, Fischer-Le Saux M, Portier P, Jacques M A, Gagnevin L, Pruvost O, Lauber E, Arlat M, Carrère S, Koebnik R, Noël L D. 2015. Genomics and transcriptomics of *Xanthomonas campestris* species challenge the concept of core type III effectome. *BMC Genomics*, **16**, 975.
Ruan J J, Zhou Y X, Zhou M L, Yan J, Khurshid M, Weng W F, Cheng J P, Zhang K X. 2019. Jasmonic acid signaling pathway in plants. *International Journal of Molecular Sciences*, **20**, 2479.
Schulze S, Kay S, Büttner D, Egler M, Eschen-Lippold L, Hause G, Krüger A, Lee J, Müller O, Scheel D, Szczesny R, Thieme F, Bonas U. 2012. Analysis of new type III effectors from *Xanthomonas* uncovers XopB and XopS as suppressors of plant immunity. *New Phytologist*, **195**, 894–911.
Sinha D, Gupta M K, Patel H K, Ranjan A, Sonti R V. 2013. Cell wall degrading enzyme induced rice innate immune responses are suppressed by the type 3 secretion system effectors XopN, XopQ, XopX and XopZ of *Xanthomonas oryzae* pv. *oryzae*. *PLoS ONE*,

8, e75867.
Song C F, Yang B. 2010. Mutagenesis of 18 type III effectors reveals virulence function of XopZ(PXO99) in *Xanthomonas oryzae* pv. *oryzae*. *Molecular Plant-Microbe Interactions*, **23**, 893–902.
Spoel S H, Dong X N. 2008. Making sense of hormone crosstalk during plant immune responses. *Cell Host Microbe*, **3**, 348–351.
Teper D, Sunitha S, Martin G B, Sessa G. 2015. Five *Xanthomonas* type III effectors suppress cell death induced by components of immunity-associated MAP kinase cascades. *Plant Signaling and Behavior*, **10**, e1064573.
Thomma B P, Eggermont K, Penninckx I A, Mauch-Mani B, Vogelsang R, Cammue B P, Broekaert W F. 1998. Separate jasmonate-dependent and salicylate-dependent defense-response pathways in *Arabidopsis* are essential for resistance to distinct microbial pathogens. *Proceedings of the National Academy of Sciences of the United States of America*, **95**, 15107–15111.
Tuttle A R, Trahan N D, Son M S. 2021. Growth and maintenance of *Escherichia coli* laboratory strains. *Current Protocols*, **1**, e20.
Tyler B M. 2017. The fog of war: How network buffering protects plants' defense secrets from pathogens. *PLoS Genetics*, **13**, e1006713.
Wang L L, Xu G J, Li L H, Ruan M Y, Bennion A, Wang G L, Li R, Qu S H. 2023. The OsBDR1-MPK3 module negatively regulates blast resistance by suppressing the jasmonate signaling and terpenoid biosynthesis pathway. *Proceedings of the National Academy of Sciences of the United States of America*, **120**, e2211102120.
Wang S F, Sun J H, Fan F G, Tan Z Y, Zou Y M, Lu D P. 2016. A *Xanthomonas oryzae* pv. *oryzae* effector, XopR, associates with receptor-like cytoplasmic kinases and suppresses PAMP-triggered stomatal closure. *Science China* (Life Sciences), **59**, 897–905.
Wang S Z, Li S, Wang J Y, Li Q, Xin X F, Zhou S, Wang Y P, Li D Y, Xu J Q, Luo Z Q, He S Y, Sun W X. 2021. A bacterial kinase phosphorylates OSK1 to suppress stomatal immunity in rice. *Nature Communications*, **12**, 5479.
Wasternack C, Hause B. 2013. Jasmonates: Biosynthesis, perception, signal transduction and action in plant stress response, growth and development. An update to the 2007 review in Annals of Botany. *Annals of Botany*, **111**, 1021–1058.
White F F, Potnis N, Jones J B, Koebnik R. 2009. The type III effectors of *Xanthomonas*. *Molecular Plant Pathology*, **10**, 749–766.
Xu Z Y, Xu X M, Gong Q, Li Z Y, Li Y, Wang S, Yang Y Y, Ma W X, Liu L Y, Zhu B, Zou L F, Chen G Y. 2019. Engineering broad-spectrum bacterial blight resistance by simultaneously disrupting variable TALE-binding elements of multiple susceptibility genes in rice. *Molecular Plant*, **12**, 1434–1446.
Xu Z Y, Xu X M, Wang Y J, Liu L L, Li Y, Yang Y, Liu L Y, Zou L F, Chen G Y. 2022. A varied AvrXa23-like TALE enables the bacterial blight pathogen to avoid being trapped by *Xa23* resistance gene in rice. *Journal of Advanced Research*, **42**, 263–272.
Yamada S, Kano A, Tamaoki D, Miyamoto A, Shishido H, Miyoshi S, Taniguchi S, Akimitsu K, Gomi K. 2012. Involvement of OsJAZ8 in jasmonate-induced resistance to bacterial blight in rice. *Plant and Cell Physiology*, **53**, 2060–2072.
Yamaguchi K, Yamada K, Ishikawa K, Yoshimura S, Hayashi N, Uchihashi K, Ishihama N, Kishi-Kaboshi M, Takahashi A, Tsuge S, Ochiai H, Tada Y, Shimamoto K, Yoshioka H, Kawasaki T. 2013. A receptor-like cytoplasmic kinase targeted by a plant pathogen effector is directly phosphorylated by the chitin receptor and mediates rice immunity. *Cell Host Microbe*, **13**, 347–357.
Yan C, Xie D X. 2015. Jasmonate in plant defence: Sentinel or double agent? *Plant Biotechnology Journal*, **13**, 1233–1240.
You Q Y, Zhai K R, Yang D L, Yang W B, Wu J N, Liu J Z, Pan W B, Wang J J, Zhu X D, Jian Y K, Liu J Y, Zhang Y Y, Deng Y W, Li Q, Lou Y G, Xie Q, He Z H. 2016. An E3 ubiquitin ligase-BAG protein module controls plant innate immunity and broad-spectrum disease resistance. *Cell Host Microbe*, **20**, 758–769.
You X M, Zhu S S, Sheng H W, Liu Z, Wang D, Wang M, Xu X, He F, Fang H, Zhang F, Wang D B, Hao Z Y, Wang R Y, Xiao Y H, Wan J M, Wang G L, Ning Y S. 2023. The rice peroxisomal receptor PEX5 negatively regulates resistance to rice blast fungus *Magnaporthe oryzae*. *Cell Reports*, **42**, 113315.
Yu G, Derkacheva M, Rufian J S, Brillada C, Kowarschik K, Jiang S S, Derbyshire P, Ma M M, DeFalco T A, Morcillo R J L, Stransfeld L, Wei Y L, Zhou J M, Menke F L H, Trujillo M, Zipfel C, Macho A P. 2022. The *Arabidopsis* E3 ubiquitin ligase PUB4 regulates BIK1 and is targeted by a bacterial type-III effector. *The EMBO Journal*, **41**, e107257.
Yuan M H, Jiang Z Y, Bi G Z, Nomura K, Liu M H, Wang Y P, Cai B Y, Zhou J M, He S Y, Xin X F. 2021. Pattern-recognition receptors are required for NLR-mediated plant immunity. *Nature*, **592**, 105–109.
Zhai K R, Deng Y W, Liang D, Tang J, Liu J, Yan B X, Yin X, Lin H, Chen F D, Yang D D, Xie Z, Liu J Y, Li Q, Zhang L, He Z H. 2019. RRM transcription factors interact with NLRs and regulate broad-spectrum blast resistance in rice. *Molecular Cell*, **74**, 996–1009.
Zhang R X, Ge S C, He J , Li S C, Hao Y H, Du H, Liu Z M, Cheng R, Feng Y Q, Xiong L Z, Li C Y, Hetherington A M, Liang Y K. 2019. BIG regulates stomatal immunity and jasmonate production in *Arabidopsis*. *New Phytologist*, **222**, 335–348.
Zhou H B, Liu B, Weeks D P, Spalding M H, Yang B. 2014. Large chromosomal deletions and heritable small genetic changes induced by CRISPR/Cas9 in rice. *Nucleic Acids Research*, **42**, 10903–10914.

Executive Editor-in-Chief Fanghao Wan
Managing Editor Juan Zhang